Journal of Medicinal Chemistry

Article

pubs.acs.org/jmc

Design, Optimization, and Biological Evaluation of Novel Keto-Benzimidazoles as Potent and Selective Inhibitors of Phosphodiesterase 10A (PDE10A)

Essa Hu,*[,†] Roxanne K. Kunz,[†] Ning Chen,[†] Shannon Rumfelt,[†] Aaron Siegmund,[†] Kristin Andrews,[‡] Samer Chmait,[‡] Sharon Zhao,[‡] Carl Davis,[§] Hang Chen,[⊥] Dianna Lester-Zeiner,[⊥] Ji Ma,[∥] Christopher Biorn,[⊥] Jianxia Shi,[∥] Amy Porter,[⊥] James Treanor,[#] and Jennifer R. Allen[†]

[†]Department of Medicinal Chemistry, [‡]Department of Molecular Structure, [§]Department of Pharmacokinetics and Drug Metabolism, [∥]Department of Neuroscience, Amgen Inc., One Amgen Center Drive, Thousand Oaks, California 91320-1799, United States

[⊥]Department of Neuroscience and [#]Department of Pharmacokinetics and Drug Metabolism, Amgen Inc., 1120 Veterans Boulevard, South San Francisco, California 94080, United States

Supporting Information

ABSTRACT: Our development of PDE10A inhibitors began with an HTS screening hit (**1**) that exhibited both high p-glycoprotein (P-gp) efflux ratios in rat and human and poor metabolic stability. On the basis of cocrystal structure of **1** in human PDE10A enzyme, we designed a novel keto-benzimidazole **26** with comparable PDE10A potency devoid of efflux liabilities. On target in vivo coverage of PDE10A in rat brain was assessed using our previously reported LC-MS/MS receptor occupancy (RO) technology. Compound **26** achieved 55% RO of PDE10A at 30 mg/kg po and covered PDE10A receptors in rat brain in a dose-dependent manner. Cocrystal structure of **26** in PDE10A confirmed the binding mode of the novel scaffold. Further optimization resulted in the identification of keto-benzimidazole **34**, which showed an increased in vivo efficacy of 57% RO in rats at 10 mg/kg po and an improved in vivo rat clearance and oral bioavailability.

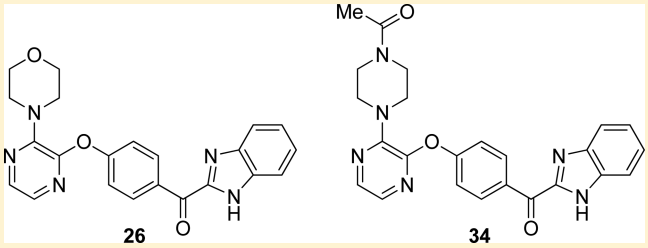

INTRODUCTION

A significant unmet medical need still exists in the treatment of schizophrenia. The current standard of care (SOC) does not address all three major symptoms of schizophrenia (positive, negative, and cognitive symptoms). While a subpopulation of patients remains unresponsive to SOC, others struggle with intolerable side effects.[1−3] As the research community searches for new approaches and mechanisms to treat schizophrenia,[4−9] inhibition of phosphodiesterase 10A (PDE10A) has emerged as a potential novel solution to address this unmet medical need. Unlike most atypical antipsychotics which directly target dopamine receptors, PDE10A regulates the levels of second messenger cyclic adenosine monophosphate (cAMP) and cyclic guanosine monophosphate (cGMP) in the signaling pathway downstream of the dopamine receptors.[10] The PDE10A enzyme is also highly expressed in the medium spiney neuron of the striatum, the section of the brain most associated with schizophrenia.[11,12] These attributes have led to the hypothesis that PDE10A modulators could offer an efficacious treatment of schizophrenia devoid of the undesired side effects of current SOC because they would not directly interact with the dopaminergic receptors. In addition, PDE10A is also reported to be downstream of the glutamine pathway, which has been postulated to be responsible for the cognitive deficits of schizophrenic patients.[13,14] Thus, inhibition of PDE10A could have the additional benefit of addressing multiple symptoms of schizophrenia unlike the current SOC. On the basis of these compelling biological findings, we sought to design potent, efficacious, and selective compounds to inhibit PDE10A in the striatum.

Traditionally, measuring drug levels in the brain homogenate or cerebrospinal fluid (CSF) has been used to assess target coverage in the central nervous system (CNS). However, because these levels could not distinguish specific from nonspecific binding in the brain, this approach could not provide definitive proof of an on-target effect. We recently described the development of a PDE10A tracer, AMG-7980, to enable measurement of PDE10A receptor occupancy (RO) in a rat brain using in vivo LC-MS/MS technology.[15] In this report, we used this technology to evaluate the effectiveness of target coverage of drug candidates and successfully identified several potent in vivo inhibitors of PDE10A in the brain.

An internal HTS screening campaign revealed compound **1** as a potent hit (IC_{50} = 9.7 nM) with acceptable average permeability in LLCK-PK1 cells of 18.1 μcm/s (Figure 1). However, the compound also exhibited several undesirable attributes: (1) sub-μM off-target kinase activities against Aurora

Received: August 8, 2013
Published: October 8, 2013

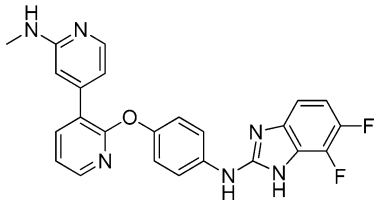

Figure 1. Initial HTS screening hit **1**.

1 and Aurora 2 kinases, high efflux ratio (ER) of 24.8 in human and 13.1 in rat, and modest to poor in vitro liver microsomal clearance in human (HLM = 127 μL/min/mg) and rat (RLM = 297 μL/min/mg). Because we were targeting the PDE10A receptors in the brain, high efflux ratios could significantly impair a drug's ability to penetrate the blood–brain barrier (BBB).[16] Furthermore, excessive systemic exposure needed to compensate for the poor CNS penetration would pose an unnecessary drug load burden on the patients. Thus, we decided to address the efflux issue first.

CHEMISTRY

As shown in Scheme 1, syntheses of aminobenzimidazoles **5** and **7** began with a S_NAr displacement of 4-aminophenol (**3**) with fluoropyridine (**2a**) or dichloropyrazine (**2b**). Aminobenzimidazoles (**5**, **6**) were formed by cyclization with di-2-pyridyl-thionocarbonate or thiophosgene and benzene-1,2-diamine. S_NAr displacement of chloropyrazine benzimidazole **6** with morpholine afforded **7**.

Synthesis of *N*-(4-((3-morpholinopyrazin-2-yl)oxy)phenyl)-benzo[*d*]thiazol-2-amine (**10**) began with coupling of morpholine with dichloropyrazine (**2a**) to form 4-(3-chloropyrazin-2-yl)morpholine (**8**) (Scheme 2). S_NAr displacement of pyrazine chloride (**8**) with 4-aminophenol (**3**) produced 4-((3-morpholinopyrazin-2-yl)oxy)aniline (**9**). Palladium catalyzed heteroaryl coupling with 2-bromobenzo[d]thiazole gave desired analog **10**.

As shown in Scheme 3, synthesis of *N*-(4-((3-morpholinopyrazin-2-yl)oxy)phenyl)pyridin-2-amine **16** began with Buchwald coupling of 1-bromo-4-methoxybenzene (**11**) to pyridin-2-amine (**12**) to afford the diaryl-aniline core (**13**). Cleavage of the methyl ether by boron tribromide revealed phenol **14**. Sequential S_NAr displacement of dichloropyrazine **2b** with phenol **14**, followed by a second S_NAr reaction to replace the remaining chlorine atom on pyrazine **15** with morpholine produced pyrazine aminopyridine **16**.

Synthesis of keto-benzthiazole **22** began with alkylation of methyl 4-hydroxybenzoate **17** with benzyl bromide to produce methyl 4-(benzyloxy)benzoate **18** (Scheme 4). Nucleophilic addition of lithium benzothiolate afforded keto-benzthiazole **19**. Deprotection with boron trifluoride revealed phenol **20**. Chloropyrazine keto-benzthiazole **21** was prepared via S_NAr displacement of phenol **20** with dichloropyrazine **2a**. Heating with morpholine resulted in formation of benzo[*d*]thiazol-2-yl(4-((3-morpholinopyrazin-2-yl)oxy)phenyl)methanone **22**.

Preparation of keto-benzimidazoles **26** and **27** started with S_NAr reaction of dichloropyrazine **2a** and ethyl 4-hydroxybenzoate **23** (Scheme 5). A one-pot, two-step reaction formed (1*H*-benzo[*d*]imidazol-2-yl)(4-((3-chloropyrazin-2-yl)oxy)-phenyl)methanone **25**. The reaction sequence began with acid catalyzed cyclization of benzene-1,2-diamine to form 1*H*-benzo[*d*]imidazole. LDA was then added to the reaction mixture to enable nucleophilic addition of 1*H*-benzo[*d*]-imidazole to ethyl 4-((3-chloropyrazin-2-yl)oxy)benzoate **24** to produce **25**. Synthesis of (1*H*-benzo[*d*]imidazol-2-yl)(4-((3-morpholinopyrazin-2-yl)oxy)phenyl)methanone **26** was accomplished by S_NAr displacement of chloropyrazine **25** with morpholine. Alkylation of imidazole amine with iodomethane produced (1-methyl-1*H*-benzo[*d*]imidazol-2-yl)(4-((3-morpholinopyrazin-2-yl)oxy)phenyl)methanone **27**. Keto-benzimidazoles **28**–**37** were synthesized in similar S_NAr reactions by combining various cyclic amines with chloropyrazine keto-benzimidazole intermediate **25** (Scheme 6).

RESULTS AND DISCUSSION

A cocrystal structure of screening hit **1** in human PDE10A enzyme's catalytic domain was first obtained to help elucidate critical binding interactions (Figure 2). The internal pyridine ring appeared to be held in place by π-stacking interactions with Ph719 and Ph686. The nitrogen atom on the internal pyridine ring was further anchored by hydrogen bonding interactions with Gln716. A second hydrogen bonding interaction between one of the nitrogens on the benzimidazole ring and Tyr683 induced a coplanar orientation of benzimidazole ring relative to the middle phenyl ring. A water molecule was resolved coordinating the benzimidazole N–H bond, while the N–H bond on the amino linker appeared to be oriented toward the solvent exposed region. Thus, neither N–H bonds seemed to

Scheme 1. Synthesis of Amino Phenyl Ether Analogs 5 and 7[a]

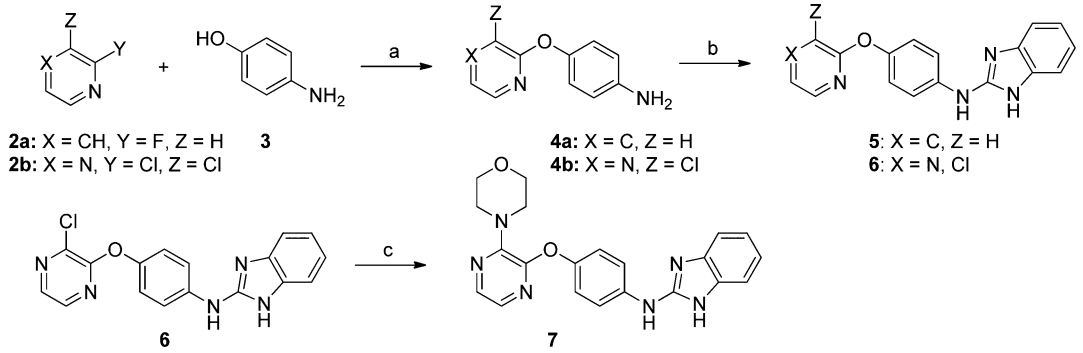

[a]Reagents and conditions: (a) cesium carbonate, DMSO, 80 °C, 16 h, 94% yield for 4a; (b) method A, (i) di-2-pyridyl-thionocarbonate, DCM, room temperature, 16 h, 18% yield for **5**; method B, (i) thiophosgene, sodium carbonate, room temperature $CHCl_3$, (ii) DCC, benzene-1,2-diamine, THF, 75 °C, 78% yield for **6**; (c) morpholine, DMSO, 80 °C, 16 h, 34% yield.

dx.doi.org/10.1021/jm401234w | J. Med. Chem. 2013, 56, 8781–8792

Scheme 2. Synthesis of Amino Phenyl Ether Analog 10[a]

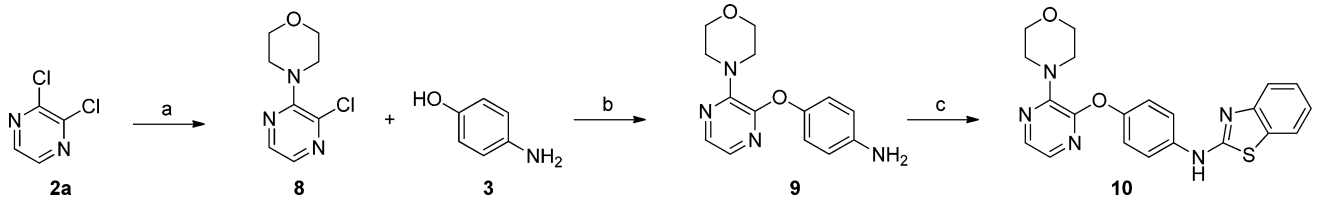

[a]Reagents and conditions: (a) morpholine, DMSO, 120 °C, 16 h, 40% yield; (b) cesium carbonate, DMSO, 80 °C, 16 h; (c) $Pd_2(dba)_3$, S-phos, sodium *tert*-butoxide, 2-bromobenzo[d]thiazole, toluene, 80 °C, 5% yield.

Scheme 3. Synthesis of Aminopyridine Analog 16[a]

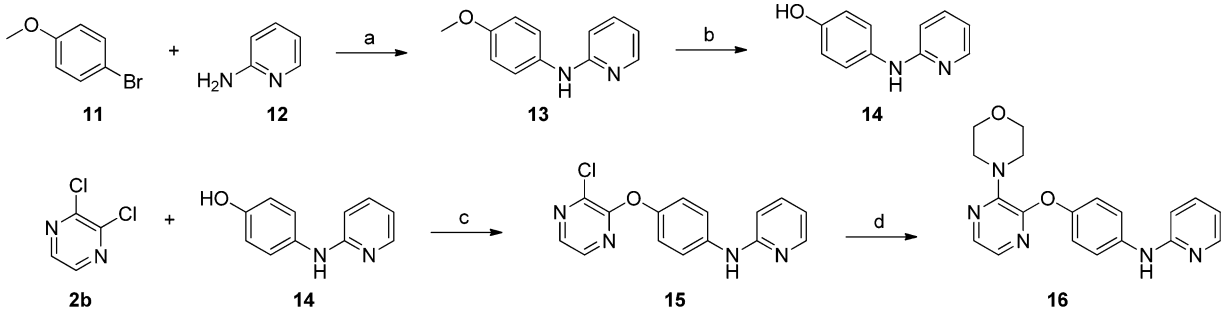

[a]Reagents and conditions: (a) $Pd_2(dba)_3$, di-*tert*-butyl(2′,4′,6′-triisopropylbiphenyl-2-yl)phosphine, sodium *tert*-butoxide, toluene, 100 °C, 3 h; (b) BBr_3, DCM, −78 °C to room temperature, 3 h, 70% yield; (c) cesium carbonate, DMF, 100 °C, 16 h, 72% yield; (d) morpholine, DMSO, 70 °C, 16 h, 80% yield.

Scheme 4. Synthesis of Keto-benzimidazole Analog 22[a]

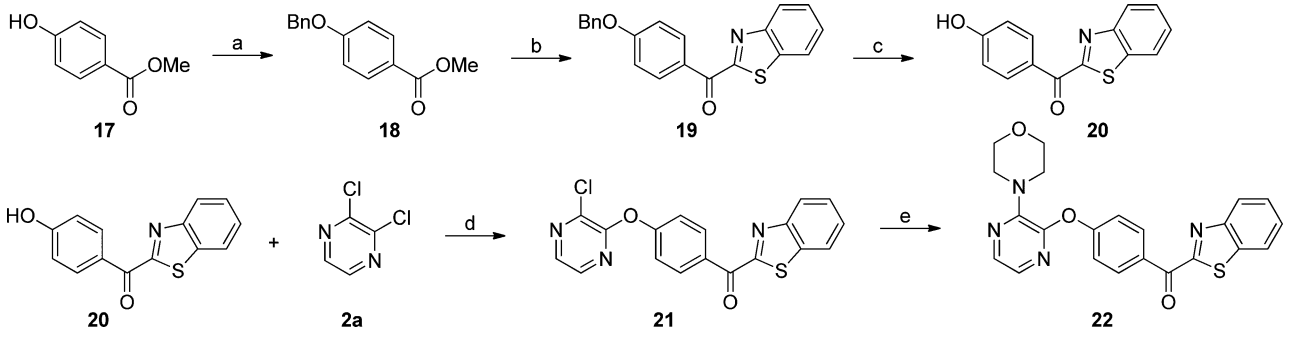

[a]Reagents and conditions: (a) potassium carbonate, benzyl bromide, DMF, room temperature, 8 h, 89% yield; (b) benzothiazole, LDA, −70 °C, 2 h, 46% yield; (c) boron trifluoride diethyl etherate, dimethyl sulfide, DCM, room temperature 72 h, 72% yield; (d) cesium carbonate, DMSO, 90 °C, 6 h, 52% yield; (e) morpholine, DMSO, 100 °C, 16 h, 57% yield.

have a critical function in the binding to the catalytic domain of PDE10A.

To eliminate the high efflux ratio, we adopted a systematic approach to investigate the structure−activity relationship of this new scaffold while retaining the key interactions observed in the PDE10A cocrystal structure (Table 1). The truncated substructure **5** was synthesized to assess the impact of the methyl-amino-pyridine functionality on screening hit **1**. Interestingly, without the methyl-amino-pyridine functionality and the two fluorine atoms on **1**, pyridine ether **5** only lost its PDE10A inhibitory activity by 5-fold while its efflux ratio improved significantly to 4.9 in rat and 4.7 in human. Furthermore, the pyridine ring could also be replaced with a pyrimidine ring with little impact on potency (data not shown). Substitution of the pyridine ring on **1** with morpholine produced **7**, which resulted in a decrease of the efflux ratios to 11.1 in human but an increase of efflux ratio to 32.8 in rat. This modification, however, brought two improvements: its PDE10A potency improved by 9-fold (IC_{50} = 1.1 nM) and the off-target Aurora 1 and 2 kinase activities of screening hit **1** were completely eliminated. Thus, we turned our attention to the rest of the scaffold to address the efflux issue while keeping the morpholine functionality in hopes of retaining its beneficial effects.

We recently reported that replacement of the N−H proton on a benzimidazole containing scaffold significantly lowered its efflux ratio.[17] Because our cocrystal structure of **1** in PDE10A enzyme seemed to suggest the benzimidazole N−H on **1** was not critical for binding, we decided to apply this strategy and replaced benzimidazole with benzthiazole (**10**) and pyridine (**16**). Indeed, compound **10** produced acceptable efflux ratios of 2.4 in human and 2.1 rat. This modification also retained comparable potency against PDE10A (IC_{50} = 4.3 nM). However, its in vitro rat clearance remained high. Efflux ratios of pyridine **16** also improved significantly to 3.7 in human and 2.6 in rat. Nevertheless, the pyridyl replacement also decreased

dx.doi.org/10.1021/jm401234w | J. Med. Chem. 2013, 56, 8781−8792

Scheme 5. Synthesis of Keto-benzimidazoles 26 and 27[a]

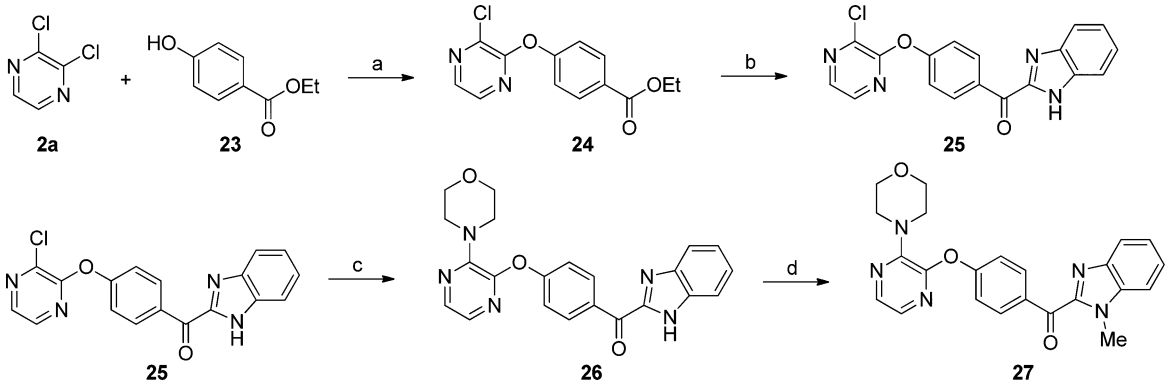

[a]Reagents and conditions: (a) cesium carbonate, DMSO, 80 °C, 16 h, 79% yield; (b) (i) benzene-1,2-diamine, triethoxymethane, benzenesulfonic acid, toluene, reflux, (ii) LDA, −78 °C→ 23 °C, 41% yield; (c) morpholine, DMSO, 80 °C, 16 h, 59% yield; (d) cesium carbonate, iodomethane, DMF, room temperature, overnight, 75% yield.

Scheme 6. Synthesis of Keto-benzimidazoles 28−37[a]

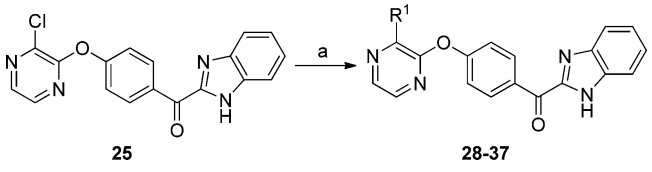

[a]Reagents and conditions: (a) cyclic amine, DMSO, 80 °C, 16 h.

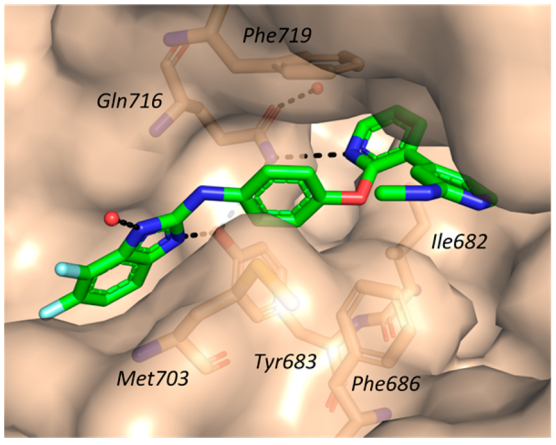

Figure 2. Cocrystal structure of **1** in human PDE10A enzyme.

the PDE10A inhibitory activity of **16** by more than 30-fold compared to **7**.

Because the cocrystal structure of **1** in PDE10A suggested that the N−H bond on the amine linker was not essential, we replaced the amine linker on **7** and **10** with a carbonyl group and synthesized **22** and **26** to maintain the planarity of the phenyl and the benzimidazole ring observed in the cocrystal structure. In several aspects, ketone replacement was detrimental to the benzthiazole analog. Compared to amino-benzthiazole **10**, keto-benzthiazole **22** was more than 30-fold less potent with higher in vitro microsomal clearance in human and rat. Keto-benzimidazole **26**, on the other hand, showed just slightly reduced PDE10A potency compared to its amino-benzimidazole analog **7**. Unlike all the previous analogs, keto-benzimidazole **26** was the first compound to exhibit both low efflux ratio (human ER = 0.9; rat ER = 1.0) and low in vitro microsomal clearance (HLM = 55 μL/min/mg; RLM = 178 μL/min/mg) in both species. *N*-Methylated benzimidazole **27** resulted in a 3-fold loss in potency, increased efflux ratio, and in vitro clearance compared to **26**. It is worth noting that there appeared to be a trend correlating cLogP with low efflux ratio. Of the five compounds with cLogP values less than 4 (compounds **7**, **16**, **22**, **26**, and **27**), four exhibited efflux ratios of 4 or less in both species.

To confirm our design hypothesis, a second cocrystal structure of keto-benzimidazole **26** in human PDE10A enzyme was obtained (Figure 3). The cocrystal structure confirmed that the new keto-benzimidazole scaffold maintained the coplanarity of middle phenyl ring and benzimidazole ring. Essential hydrogen bonding interactions (pyrimidine nitrogen with Gln716, benzimidazole nitrogen with Tyr683) and π-stacking interactions (pyrimidine with Ph719 and Phe686) previously observed in cocrystal structure of **1** in PDE10A enzyme (Figure 2) were also retained.

To assess whether our SAR efforts were on track, compound **26** was advanced into the LC-MS/MS RO assay recently reported by our group to assess its CNS target coverage in vivo.[1] Using our reported PDE10A tracer AMG-7980, we were gratified to see that keto-benzimidazole **26** produced 21% RO at 10 mg/kg and 55% RO at 30 mg/kg. Compared to high in vivo rat clearance of screening hit **1** (3.90 L/h/kg), compound **26** achieved modest clearance of 0.53 L/h/kg and good $T_{1/2}$ (3.19 h), albeit a low oral bioavailability (10%*F*). Dose dependent occupancy of CNS PDE10A receptors by **26** was also evaluated using LC-MS/MS RO dose response assay at 0.3, 1, 3, 10, and 30 mg/kg doses. Poor oral bioavailability of **26** was circumvented by dosing the compound ip instead. Occupancy measurements were taken 30 min post dosing. As shown in Figure 4, keto-benzimidazole **26** exhibited an increase in PDE10A occupancy in the rat brain in vivo in a dose dependent manner. This in vivo validation of the keto-benzimidazole scaffold provided the critical data we needed to continue to optimize lead compound **26**.

To address the poor PKDM profile of **26**, we initiated an investigation of structure−activity relationship of the morpholine region. To further expedite our discovery timeline, our LC-MS/MS RO technology platform was set up to handle multiple compounds a week with short turnaround time. This enabled us to advance compounds that exhibited acceptable in vitro PDE10A inhibitory activity and in vitro metabolic stability directly into the LC-MS/MS RO studies instead of the

dx.doi.org/10.1021/jm401234w | J. Med. Chem. 2013, 56, 8781−8792

Table 1. Structural Modifications to Reduce Efflux Ratio of Screening Hit 1

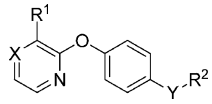

cmpd	R^1	X	Y	R^2	PDE10A IC_{50} (nM)[a]	Human Efflux Ratio[b]	Rat Efflux Ratio[b]	HLM (μL/min/mg)[c]	RLM (μL/min/mg)[c]	cLogP
1		CH	NH	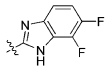	9.7±0.86	24.8	13.1	127	297	5.45
5	H	CH	NH		45.0±1.6	4.9	4.7	17	>399	4.62
7		N	NH		1.1±0.02	11.1	32.8	51	>399	3.86
10		N	NH		4.3±0.42	2.4	2.1	57	320	4.45
16		N	NH		36.6±1.3	3.7	2.6	33	204	2.94
22		N	C(O)		168±5.7	4.1	3.4	775	628	3.74
26		N	C(O)		4.5±0.44	0.9	1.0	55	178	3.28
27		N	C(O)		12.5±0.49	3.2	3.9	156	644	3.22

[a]Each IC_{50} value reported is an average of at least two independent experiments with 22 point dose response curve in duplicates at each concentration. [b]Efflux ratio reported is based on the ratio of the basolateral to apical permeability over apical to basolateral permeability of a compound. MDR1−Madin−Darby canine kidney (MDCK) cells were used to measure the compound's apparent permeability in each direction. [c]In vitro microsomal stability studies were conducted in the presence of NADPH at 37 °C for 30 min at a final compound concentration of 1 μM of compound.

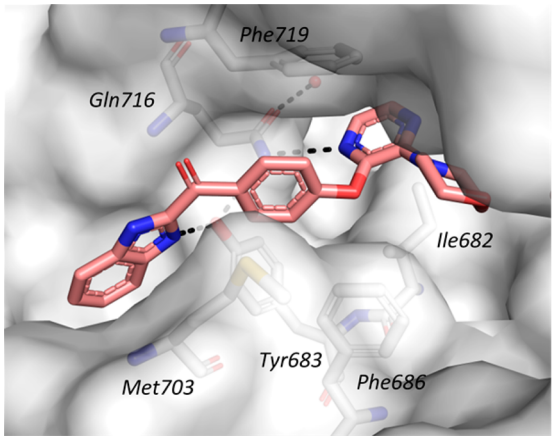

Figure 3. Cocrystal structure of **26** in human PDE10A enzyme.

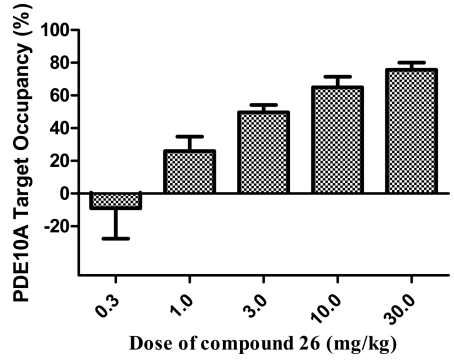

Figure 4. Dose dependent increase in PDE10A receptor occupancy in CNS observed for keto-benzimidazole **26**.

traditional order of rat PK before in vivo PD studies. Using LC-MS/MS RO technology to filter out compounds also significantly reduced the number of in vivo rat PK studies we needed to support the project advancement.

A variety of N-linked rings were synthesized to examine the effects of electronics and ring sizes on the in vitro metabolic stability of the keto-benzimidazole scaffold (Table 2).

dx.doi.org/10.1021/jm401234w | J. Med. Chem. 2013, 56, 8781−8792

Table 2. Modification of the Morpholine Ring

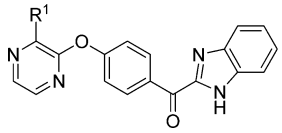

Cmpd#	R^1	PDE10A IC_{50} (nM)[a]	HLM (μL/min/mg)[b]	RLM (μL/min/mg)[b]
26		4.5±0.44	55	178
28		7.4±0.22	213	477
29		5.1±0.52	52	440
30		20.6±2.6	73	243
31		7.2±0.54	128	509
32		4.1±0.33	57	236
33	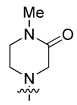	1.7±0.07	20	122
34	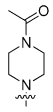	5.1±0.64	33	108
35	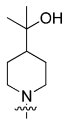	2.8±0.35	152	579
36	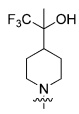	24.4±4.2	88	>399

[a]Each IC_{50} value reported is an average of at least two independent experiments with 22 point dose response curve in duplicates at each concentration. [b]In vitro microsomal stability studies were conducted in the presence of NADPH at 37 °C for 30 min at final compound concentration of 1 μM of compound.

Compared to morpholine **26**, piperidine **28**, with one atom difference, showed comparable potency but increased in vitro microsomal clearance in human and rat. Increasing the ring size (**29**) did not impact PDE10A potency but significantly increased RLM. *N*-Methyl piperazine **30** exhibited a modest 4-fold decrease in activity while its in vitro metabolic stability increased slightly in both human and rat. 4-Methoxy piperidine (**31**) showed comparable potency to morpholine **26** but higher in vitro clearance in both species. Replacing the methyl ether with an alcohol (**32**) did not impact PDE10A activity but slightly increased RLM. Interestingly, insertion of a carbonyl group α to the distal piperidine nitrogen (**33**) increased its inhibitory activity against PDE10A to single digit nM (IC_{50} = 1.7 nM) compared to its *N*-methyl-piperazine analog **30**. The polar functional group also restored in vitro clearance in both species (HLM = 20 μL/min/mg; RLM = 122 μL/min/mg). This improvement in binding affinity was likely due to the carbonyl group making a hydrogen bonding interaction with one of the water molecules occupying the solvated metal binding pocket in the PDE10A catalytic domain.[18] To further exploit this finding, we proceeded to install various oxygen containing polar groups on the N-linked six-membered ring. *N*-Acetyl piperazine **34** did not experience the potency increase observed with **33** even though its HLM and RLM profiles improved slightly. Compared to the secondary alcohol on piperidinol **32**, tertiary alcohol (**35**) was similarly potent but exhibited significantly higher in vitro clearance in rat. Changing the electronic property of the alcohol by replacing one of the *gem*-dimethyl groups with a trifluoromethyl group (**36**) resulted in 8-fold loss in activity against PDE10A.

On the basis of their respective in vitro PDE10A inhibitory potency and in vitro metabolic stability in both human and rat, compounds **32**, **33**, and **34** were advanced into the LC-MS/MS RO assays (Table 3). Piperidinol **32** was more efficacious in vivo than **26**, exhibiting 39% RO when dosed at 10 mg/kg po. Piperazinone **33** was not able to cover the PDE10A receptors in the rat brain (RO = 0% at 10 mg/kg). Acetyl piperidine **34**, which had comparable PDE10A potency as **26** but reduced in vitro clearance in rat, produced an improved in vivo occupancy of 57% RO at 10 mg/kg po in the LC-MS/MS RO assay.

Table 3. Receptor Occupancy Measurements of Keto-benzimidazoles 26, 32, 33, and 34 Using ex Vivo and LC-MS/MS Methods

compd no.	LC-MS/MS receptor occupancy (%)[a]
26	21.3
	55.3[b]
32	39.4
33	0
34	57.1

[a]Receptor occupancy measurements were taken 1 h post po dosing of compounds at 10 mg/kg. [b]1 h post po dosing of compound at 30 mg/kg.

Compared to high in vivo rat clearance of screening hit **1** (3.90 L/h/kg) and the poor oral bioavailability of compound **26** (10%*F*), keto-benzimidazoles **32** and **34** exhibited improved in vivo rat PK profiles (Table 4). Compound **32** afforded improved oral bioavailability of 52% even though it was inferior to **26** in terms of in vivo clearance (1.10 L/h/kg) and $T_{1/2}$ (1.96 h). Meanwhile, compound **34** showed the best overall improvement with a low in vivo clearance of 0.074 L/h/kg, good $T_{1/2}$ of 3.9 h, and acceptable oral bioavailability of 56%.

CONCLUSION

HTS screening hit **1** was identified as a potent inhibitor of PDE10A (IC_{50} = 9.7 nM). The molecule displayed high efflux ratios in both human and rat, as well as high in vitro and in vivo clearance in rat and off-target kinase activities. Cocrystal structure of **1** in human PDE10A catalytic domain revealed two key interactions: binding of pyridine nitrogen to the conserved

dx.doi.org/10.1021/jm401234w | J. Med. Chem. 2013, 56, 8781−8792

Table 4. In Vivo Rat PK of Compounds 1, 26, 32, and 34[a]

compd no.	route[b]	dose (mg/kg)	Cl (L/h/kg)	Vss (L/kg)	AUC (μM·h)	$T_{1/2}$ (h)	%F
1	iv	1	3.90	2.52	0.58	0.81	
26	iv	2	0.53	1.35	9.32	2.63	
	po	5			4.35	3.19	10
	ip	10	1.40	27.6	12.10	20.4	
32	iv	2	1.10	1.28	4.50	4.21	
	po	10			11.70	1.96	52
34	iv	2	0.074	0.165	62.10	1.65	
	po	5			79.2	3.90	56

[a]Study in fed male Sprague−Dawley rats. [b]Vehicles used: 100% DMSO for iv; 1% Tween, 2% HPMC with methanesulfonic acid, pH 2.2, for po and ip.

Gln716 and binding of imidazole nitrogen to Tyr683. While maintaining these two essential hydrogen bonding interactions, we systematically examined the remainder of the scaffold and identified keto-benzimidazole **26** as a promising new scaffold. The key bonding interactions and binding conformation of this new keto-benzimidazole scaffold was confirmed with a second cocrystal structure of **26** in human PDE10A. For proof of concept, keto-benzimidazole **26** with nM PDE10A potency and modest in vitro rat microsomal clearance was advanced into an in vivo LC-MS/MS RO studies and showed a promising 55% RO at 30 mg/kg by po dosing. Additional LC-MS/MS RO dose response study further demonstrated that **26** was able to cover the PDE10A receptors in a dose dependent manner. Modifications of the morpholine region of the scaffold to optimize metabolic stability led to identification of compound **34**. Compared to lead compound **26**, keto-benzimidazole **34** possessed a superior in vivo efficacy, achieving 57% RO at 10 mg/kg po in the LC-MS/MS RO assay. In addition, **34** exhibited improved in vivo rat clearance and oral bioavailability. Both compounds **26** and **34** were highly selective for PDE10A, exhibiting 7−30 μM inhibitory activities against the remaining PDE isoforms (PDE1, 2, 3, 4, 5, 6, 7, 8, 9, and 11). Our work to further increase the in vivo efficacy of these keto-benzimidazole PDE10A inhibitors will be reported in a future communication.

EXPERIMENTAL METHODS

Chemistry, Materials, and General Methods. Unless otherwise noted, all reagents and solvents were obtained from commercial suppliers such as Aldrich, Sigma, Fluka, Acros, EDM Sciences, etc., and used without further purification. Dry organic solvents (dichloromethane, acetonitrile, DMF, etc.) were purchased from Aldrich packaged under nitrogen in Sure/Seal bottles. All reactions involving air or moisture sensitive reagents were performed under a nitrogen or argon atmosphere. Silica gel chromatography was performed using prepacked silica gel cartridges (Biotage or RediSep). Microwave assisted reactions were performed in Biotage Initiator Sixty microwave reactor. ^{1}H NMR spectra were recorded on a Bruker DRX 300 MHz, Bruker DRX 400 MHz, Bruker AV 400 MHz, Varian 300 MHz, or a Varian 400 MHz spectrometer at ambient temperature. Chemical shifts are reported in parts per million (ppm, δ units). Data are reported as follows: chemical shift, multiplicity (s = singlet, d = doublet, t = triplet, q = quartet, br = broad, m = multiplet), coupling constants, and number of protons. Reactions were monitored using Agilent 1100 series LC/MSD SL high performance liquid chromatography (HPLC) systems with UV detection at 254 nm and a low resonance electrospray mode (ESI). All final compounds were purified to >95% purity, as determined by high performance liquid chromatography (HPLC). HPLC methods used the following: Agilent 1100 spectrometer, Zorbax SB-C18 column (50 mm × 3.0 mm, 3.5 μm) at 40 °C with a 1.5 mL/min flow rate; solvent A of 0.1% TFA in water, solvent B of 0.1% TFA in MeCN; 0.0−3.0 min, 5−95% B; 3.0−3.5 min, 95% B; 3.5−3.51 min, 5% B. Flow from UV detector was split (50:50) to the MS detector, which was configured with APIES as ionizable source. All high resolution mass spectrometry (HRMS) data were acquired on a Synapt G2 HDMS instrument (Waters Corporation, Manchester, UK) operated in positive electrospray ionization mode. The sample was diluted to 10 μM in 50% acetonitrile (v/v), 0.1% formic acid (v/v), and infused into the mass spectrometer at a flow rate of 5 μL/min through an electrospray ionization source operated with a capillary voltage of 3 kV. The sample cone was operated at 30 V. The time-of-flight analyzer was operated at a resolution (fwhm) of 30000 at m/z 785 and was calibrated over the m/z range 50−1200 using a 1 μM sodium iodide (NaI) solution (50% v/v acetonitrile solution). To obtain accurate mass measurements, an internal lock-mass correction was applied using leucine enkephalin (m/z 556.2771). Collision induced fragmentation (CID) was performed using an injection voltage of 28 V. Instrument control was performed through the software suite MassLynx, version 4.1.

*4-(Pyridin-2-yloxy)benzenamine (**4a**).* To a solution of **3** (545 mg, 5.0 mmol) in DMSO (8 mL) was added cesium carbonate (1.95 g, 6.0 mmol) and **2a** (0.43 mL, 5.0 mmol). The resulting mixture was heated in an 80 °C oil bath for 16 h. After cooling to RT, the reaction mixture was diluted with DCM and washed with water and brine several times to remove DMSO. The organic layer was dried (Na_2SO_4) and concentrated to give **4a** (875 mg, 94% yield) as a tan solid. LC-MS m/z [M + H] 187.2.

*4-(3-Chloropyrazin-2-yloxy)benzenamine (**4b**).* A mixture of **2b** (470 mg, 3.16 mmol) with **3** (344 mg, 3.16 mmol) and cesium carbonate (1233 mg, 3.79 mmol) in DMSO and was heated to 70 °C for 3 h. The mixture was cooled to room temperature then transferred to a separatory funnel rinsing with ethyl acetate and water. The layers were separated, and the aqueous layer was back extracted with ethyl acetate (3×). The combined organic layers were rinsed with brine, dried over Na_2SO_4, filtered, and concentrated to produce **4b** as a solid (620 mg, 88% yield), which was carried forward without further purification. LC-MS m/z [M + H] 222.0.

*N-(4-(Pyridin-2-yloxy)phenyl)-1H-benzo[d]imidazol-2-amine (**5**).* In a round-bottomed flask were added **4a** (186 mg, 1.0 mmol), di-2-pyridyl thionocarbonate (244 mg, 1.05 mmol), and DCM (5 mL). The reaction mixture was stirred at RT for 16 h. The reaction mixture was partitioned between DCM and water. The aqueous layer was extracted with DCM, and the combined organics were washed with brine, dried (Na_2SO_4), and concentrated. The crude material was dissolved in THF (20 mL), to which was added 1,2-phenylenediamine (162 mg, 1.5 mmol) and PS-carbodiimide resin (Argonaut, 0.88 mmol/g, 3.2 g, 2.85 mmol). The reaction was heated at 70 °C for 4 h, cooled to RT, filtered, and concentrated. The crude product was dissolved in DCM and chromatographed through a Redi-Sep prepacked silica gel column (40 g), eluting with a gradient of 10−100% EtOAc in hexane, to provide **5** (55 mg, 18% yield) as off-white solid. ^{1}H NMR (400 MHz, $CDCl_3$) δ ppm 6.71 (s, 1 H), 6.96 (d, J = 8.53 Hz, 1 H), 7.00−7.06 (m, 1 H), 7.08−7.16 (m, 4 H), 7.28−7.42 (m, 4 H), 7.72 (t, J = 7.78 Hz, 1 H), 8.19 (d, J = 4.52 Hz, 1 H). LC-MS m/z [M + H] 303.2.

*N-(4-(3-Chloropyrazin-2-yloxy)phenyl)-1H-benzo[d]imidazol-2-amine (**6**).* To a mixture of **4b** (620 mg, 2.80 mmol) and sodium

dx.doi.org/10.1021/jm401234w | J. Med. Chem. 2013, 56, 8781−8792

carbonate (652 mg, 6.15 mmol) in chloroform was added thiophosgene (0.24 mL, 3.08 mmol). The solution turned cloudy and was stirred overnight at room temperature. Reaction mixture was filtered, and the filtrate was concentrated by rotovap to give a brown solid.

A mixture of 2-chloro-3-(4-isothiocyanatophenoxy)pyrazine (190 mg, 0.72 mmol), benzene-1,2-diamine (93.5 mg, 0.87 mmol), and *N*,*N*′-dicyclohexylcarbodiimide (223 mg, 1.08 mmol) in THF was heated at 75 °C for 1.5 h. The reaction mixture was cooled to room temperature, diluted with DCM, and absorbed onto silica gel for purification. Gradient elution with 20−100% EtOAc/hexanes afforded **6** as a solid (191 mg, 78% yield). LC-MS *m*/*z* [M + H] 338.0.

*N-(4-(3-Morpholinopyrazin-2-yloxy)phenyl)-1H-benzo[d]-imidazol-2-amine (**7**).* A mixture of **6** (191 mg, 0.57 mmol) and morpholine (0.074 mL, 0.85 mmol) in DMSO (2 mL) was heated to 80 °C overnight. The hot solution was then poured onto ice water, which caused a brown solid to precipitate. The solid was collected by filtration, washed, and dried to give **7** (75 mg, 34% yield). ^{1}H NMR (300 MHz, DMSO-d_6) δ ppm 3.47−3.59 (m, 4 H), 3.69−3.83 (m, 4 H), 6.89−7.06 (m, 2 H), 7.12 (m, *J* = 8.92 Hz, 2 H), 7.22−7.39 (m, 2 H), 7.55 (d, *J* = 2.63 Hz, 1 H), 7.79 (m, *J* = 8.92 Hz, 2 H), 7.90 (d, *J* = 2.78 Hz, 1 H), 9.43 (s, 1 H), 10.92 (s, 1 H). LC-MS *m*/*z* [M + H] 389.1.

*4-(3-Chloropyrazin-2-yl)morpholine (**8**).* A solution of **2a** (2.03 g, 13.63 mmol), morpholine (1.22 mL, 14.00 mmol), and toluene (10 mL) was stirred at 120 °C for 16 h. The reaction was poured into 10% Na_2CO_3 solution (20 mL) and extracted with EtOAc (2 × 30 mL). The combined organics were washed with brine and concentrated in vacuo. The crude product was adsorbed onto a plug of silica gel and chromatographed through a Redi-Sep prepacked silica gel column (40 g), eluting with 0% to 30% EtOAc in hexane, to provide **8** (1.11 g, 40.8% yield).

*4-(3-Morpholinopyrazin-2-yloxy)benzenamine (**9**).* To a 25 mL round-bottomed flask was added **8** (1.094 g, 5.5 mmol), **3** (0.60 g, 5.5 mmol), and cesium carbonate (2.25 g, 6.6 mmol) in DMSO at 80 °C. Reaction mixture was allowed to cool to room temperature, diluted with water, and extracted with CH_2Cl_2. The organic extract was washed with water and saturated NaCl solution and dried with $MgSO_4$. The concentrated residue was taken up in DCM and loaded onto SCX cartridges. The cartridges were rinsed with DCM 3×, MeOH 3×, and 2.0 M ammonia in MeOH collecting fractions during each rinse. The ammonia fractions were combined and concentrated to give **9**. LC-MS *m*/*z* [M + H] 273.2.

*N-(4-(3-Morpholinopyrazin-2-yloxy)phenyl)benzo[d]thiazol-2-amine (**10**).* A microwave reaction vessel was charged with **9** (0.109 g, 0.40 mmol), 2-bromobenzo[d]thiazole (0.074 g, 0.35 mmol), $Pd_2(dba)_3$ (0.0277 g, 0.024 mmol), 2-dicyclohexylphosphino-2′,6′-dimethoxy-1,1′-biphenyl (0.0198 g, 0.048 mmol), and sodium *t*-butoxide (0.0974 g, 1.2 mmol). The reaction mixture was stirred and heated in a Discover model microwave reactor (CEM, Matthews, NC) at 150 °C for 20 min (125 W, Powermax feature on, ramp time 10 min). Solvent was concentrated in vacuo. The crude product was purified by reverse-phase preparative HPLC using a Phenomenex Gemini column, 5 μm, 150 mm × 30 mm, 0.1% TFA in CH_3CN/H_2O, gradient 10−100% over 15 min to afford **10** (8.6 mg, 5.3% yield). ^{1}H NMR (300 MHz, $CDCl_3$) δ ppm 3.59−3.69 (m, 4 H), 3.84−3.94 (m, 4 H), 7.11−7.22 (m, 3 H), 7.35 (td, *J* = 7.75, 1.17 Hz, 1 H), 7.54−7.57 (m, 2 H), 7.57−7.59 (m, 1 H), 7.59−7.67 (m, 2 H), 7.88 (d, *J* = 2.78 Hz, 1 H). LC-MS *m*/*z* [M + H] 406.0.

*N-(4-Methoxyphenyl)pyridin-2-amine (**13**).* A solution of **11** (5.0 g, 26.7 mmol), **12** (3.58 g, 37.4 mmol, 1.4 equiv), and sodium *tert*-butoxide (7.68 g, 80 mmol, 3.0 equiv) in 50 mL of toluene was degassed by nitrogen purging for 30 min before addition of $Pd(dba)_2$ (0.541 g, 0.66 mmol, 0.025 equiv) and di-*tert*-butyl(2′,4′,6′-triisopropylbiphenyl-2-yl)phosphine (0.566 g, 1.3 mmol, 0.05 equiv). The reaction mixture was degassed for an additional 15 min before heating to 100 °C for 3 h. The mixture was cooled to room temperature and diluted with water and extracted with ethyl acetate (200 × 3 mL). The combined organic layers were filtered through Celite. The Celite cake was washed with ethyl acetate. The filtrate was dried over sodium sulfate and concentrated. Purification by column chromatography (15% ethyl acetate:hexane) produced **13**. ^{1}H NMR (DMSO-d_6): δ ppm 8.076 (d, 1H), 7.543 (d, 2H), 7.409 (m, 1H), 6.865 (d, 2H), 6.727 (d, 1H), 6.665 (m, 1H), 3.708 (s, 3H).

*4-(Pyridin-2-ylamino)phenol (**14**).* A solution of **13** (3.0 g, 14.9 mmol) in DCM (50 mL) was cooled to −78 °C before dropwise addition of BBr_3 (4.5 mL, 44.1 mmol, 3.0 equiv) under nitrogen atmosphere over 30 min. The temperature was maintained at −78 °C for 1 h before allowing to warm to room temperature over 2 h. Reaction was cooled to 0 °C and quenched with saturated sodium bicarbonate solution. The resulting mixture was stirred for 30 min and extracted by ethyl acetate (200 × 3 mL). The combined organic extracts were dried over sodium sulfate and concentrate to give **14** (1.95 g, 70.0% yield), which was used directly for next step. ^{1}H NMR (DMSO-d_6): δ ppm 9.114 (s, 1H), 8.205 (d, 2H), 8.171 (d, 1H), 7.755 (d, 2H), 7.592 (t, 1H), 7.154 (d, 2H), 6.840 (d, 1H), 6.767(t, 1H).

*N-(4-(3-Chloropyrazin-2-yloxy)phenyl)pyridin-2-amine (**15**).* A solution of **14** (10 g, 51 mmol) and **2b** (7.75 g, 81 mmol, 1.4 equiv) in DMF (100 mL) was added cesium carbonate (34.5 g, 106 mmol, 2 equiv) and heated to 100 °C overnight. Reaction mixture was concentrated under vacuum and precipitated with water. The mixture was stirred for 1 h and filtered to afford a brown solid. The solid was then washed with ether to afford **15** (11.5 g, 72% yield). ^{1}H NMR (DMSO-d_6): δ ppm 9.116 (s. 1H), 8.197 (d, 2H), 8.165 (d, 1H), 7.750 (d, 2H), 7.589 (t, 1H), 7.147 (d, 2H), 6.835 (d, 1H), 6.760 (t, 1H).

*N-(4-((3-(4-Morpholinyl)-2-pyrazinyl)oxy)phenyl)-2-pyridinamine (**16**).* A suspension of *N*-(4-((3-chloro-2-pyrazinyl)oxy)phenyl)-2-pyridinamine (285 mg, 0.95 mmol) and morpholine (0.42 mL, 4.77 mmol) in DMSO (2 mL) was heated at 70 °C for 72 h. Reaction was then partitioned between 9:1 $CHCl_3$/IPA (30 mL) and 1 M NaOH (30 mL). The separated organic layer was dried over $MgSO_4$, concentrated under reduced pressure, then purified by silica gel chromatography, eluting products with a 0−4% gradient of MeOH/CH_2Cl_2 over 20 column volumes to afford **16** (267 mg, 80% yield, 97.7% purity) as an off-white solid. ^{1}H NMR (400 MHz, DMSO-d_6) δ ppm 3.48−3.57 (m, 4 H), 3.71−3.81 (m, 4 H), 6.73 (dd, *J* = 6.65, 5.28 Hz, 1 H), 6.81 (d, *J* = 8.41 Hz, 1 H), 7.02−7.10 (m, 2 H), 7.50−7.60 (m, 2 H), 7.66−7.72 (m, 2 H), 7.89 (d, *J* = 2.74 Hz, 1 H), 8.13 (dd, *J* = 5.09, 1.37 Hz, 1 H), 9.04 (s, 1 H). LC-MS *m*/*z* [M + H] 350.1. HRMS (ES+) calcd for $[C_{19}H_{19}N_5O_2]^+$, 349.154; found, 350.162.

*4-Benzyloxy-benzoic Acid Methyl Ester (**18**).* In a 2 L two neck round-bottom flask, **17** (100 g, 657 mmol) was dissolved in 500 mL of DMF and potassium carbonate (180 g, 1300 mmol) and cooled to 0 °C. Benzyl bromide (77 mL, 657 mmol) was added dropwise for 30 min. After stirring for 8 h at room temperature, reaction mixture was diluted with 500 mL of water. The precipitated solid was filtered and washed with water to afford **18** (150 g, 89% yield). ^{1}H NMR ($CDCl_3$, 300 MHz): δ ppm 3.8 (s, 3H), 5.2 (s, 1H), 6.9 (d, 1H), 7.32 (m, 5H), 7.98 (m, 2H).

*Benzothiazol-2-yl-(4-benzyloxy-phenyl)-methanone (**19**).* In a 100 mL round-bottom flask, a mixture of **18** (0.8 g, 3.1 mmol) and benzothiazole (312 mg, 3.1 mmol) in dry THF was cooled to −70 °C. LDA (15.2 mL 1.6 M, 18.6 mmol) was added slowly for 5 min. Reaction mixture was stirred for an additional 2 h at −70 °C. Reaction mixture was quenched with 1N HCl solution and extracted with ethyl acetate, washed with brine solution, and dried over anhydrous sodium sulfate. Volatile solvents were evaporated under vacuum. The crude product was recrystallized from hexane ethyl acetate mixture to afford **19** (500 mg, 46% yield). ^{1}H NMR ($CDCl_3$, 300 MHz): δ ppm 5.2 (s, 2H), 7.1 (m, 2H), 7.34 (m, 5H), 7.5−7.6 (m, 2H), 8.0 (m, 1H), 8.22 (m, 1H), 8.62 (m, 2H).

*Benzothiazol-2-yl-(4-hydroxy-phenyl)-methanone (**20**).* In a 1 L round-bottom flask **19** (30 g, 86.9 mmol) was stirred in a solution of boron trifluoride diethyl etherate (101.2 g, 312 mmol) and dimethylsulfide (112 g, 809 mmol) in dry CH_2Cl_2 (300 mL) at room temperature for 72 h. The mixture was then quenched with water and diluted with CH_2Cl_2. The organic phase was washed with brine and dried over anhydrous Na_2SO_4. Crude product was purified by silica gel column chromatography using hexane and ethyl acetate to afford **20** (16 g, 72% yield). ^{1}H NMR ($CDCl_3$, 300 MHz): δ ppm 6.95

(s, 2H), 7.5−7.62 (m, 2H), 8.01 (m, 1H), 8.22 (m, 1H), 8.58 (m, 2H). LC-MS m/z [M + H] 256.

*Benzothiazol-2-yl-[4-(3-chloro-pyrazin-2-yloxy)-phenyl]-methanone (**21**).* In 250 mL round-bottom flask **20** (6 g, 23.5 mmol) was dissolved in DMSO (60 mL). Compound **2b** (3.48 g, 23.5 mmol) and cesium carbonate (15 g, 47 mmol) were added, and the resulting mixture was stirred at 90 °C for 6 h. Reaction mixture was diluted with cold water, and the precipitate was collected by filtration. The crude compound was purified by silica gel column chromatography to afford **21** (4.5g, 52% yield). ^{1}H NMR ($CDCl_3$, 300 MHz): δ ppm 7.35 (m, 2H), 7.5−7.62 (m, 2H), 8.01 (m, 2H), 8.13(d, 1H), 8.73 (m, 2H). LC-MS m/z [M + H] 368.

*Benzo[d]thiazol-2-yl(4-(3-morpholinopyrazin-2-yloxy)phenyl)-methanone (**22**).* To a solution of **21** (185 mg, 0.5 mmol) in DMSO (2 mL) was added morpholine (0.22 mL, 2.5 mmol). The reaction mixture was heated at 100 °C for 2 h. The reaction mixture was partitioned between EtOAc and brine. The precipitate formed was collected by filtration and washed with EtOAc and water. The solid was dried to provide **22** (120 mg, 57% yield) as light-yellow solid. ^{1}H NMR (400 MHz, DMSO-d_6) δ ppm 3.49−3.60 (m, 4 H), 3.69−3.79 (m, 4 H), 7.44 (d, J = 8.80 Hz, 2 H), 7.60−7.75 (m, 3 H), 8.04 (d, J = 2.74 Hz, 1 H), 8.26−8.37 (m, 2 H), 8.55 (d, J = 8.80 Hz, 2 H). LC-MS m/z [M + H] 419.0.

*Ethyl 4-(3-Chloropyrazin-2-yloxy)benzoate (**24**).* To a solution of **23** (11.2 g, 67.1 mmol) and **2a** (10.00 g, 67.1 mmol) in DMSO was added cesium carbonate (26.2 g, 80.5 mmol). The mixture was heated at 70 °C for 6 h. The mixture was cooled to room temperature and diluted with water and DCM, and the layers were separated and the aqueous was extracted with DCM (2×). The combined organics were washed with brine, dried over Na_2SO_4, filtered, and concentrated. The crude material was purified by Biotage, using 15−20% ethyl acetate/hexanes gradient to give **24** as a white solid (14.9g, 79% yield). LC-MS m/z [M] 278.9.

*(1H-Benzo[d]imidazol-2-yl)(4-(3-chloropyrazin-2-yloxy)phenyl)-methanone (**25**).* A solution of benzene-1,2-diamine (750 mg, 6.93 mmol), triethyl orthoformate (2.85 mL, 18.66 mmol), and benzenesulfonic acid (37 mg, 0.24 mmol) in toluene was heated to reflux for 4 h and then slowly distilled to remove half of the solvent. The mixture was then cooled to room temperature and neutralized with 0.1 mL of diisopropyl amine, followed by addition of a solution of **24** (2.13 g, 7.63 mmol) in THF (7 mL). The mixture was cooled to −78 °C, and 1.2 equiv of LDA (4.62 mL, 8.32 mmol) was added. After aging at −78 °C for 1.5 h, the mixture was warmed to room temperature after 1.5 h and then 2 N HCl solution was added. The resulting mixture was agitated for 30 min. The pH of mixture was adjusted to pH 9 with 1N NaOH solution. Ethyl acetate was added and the layers were separated. The aqueous layer was back extracted with ethyl acetate (3×), and the combined organics were washed with brine, dried over Na_2SO_4, filtered, and concentrated to give **24** (987 mg, 41% yield). LC-MS m/z [M + H] 351.0.

*(1H-Benzo[d]imidazol-2-yl)(4-(3-morpholinopyrazin-2-yloxy)-phenyl)methanone (**26**).* A solution of **25** (23.0 g, 65.6 mmol) and morpholine (17.2 mL, 197 mmol) was heated to 90 °C in DMSO. After complete consumption of the starting material, the hot solution was dripped into ice water, which caused a yellow solid to precipitate. The solid was slurried in boiling EtOH, and enough tetrahydrofuran was added to completely dissolve the solids. The solution was transferred to the freezer for crystallization. The solid was collected by filtration and air-dried to give **26** (15.5 g, 59% yield). ^{1}H NMR (300 MHz, $CDCl_3$) δ ppm 3.57−3.70 (m, 4 H), 3.79−3.95 (m, 4 H), 7.22−7.34 (m, 3 H), 7.35−7.49 (m, 2 H), 7.59 (d, J = 2.63 Hz, 1 H), 7.78 (br s, 2 H), 7.95 (d, J = 2.78 Hz, 1 H), 8.77−8.95 (m, 2 H). LC-MS m/z [M + H] 402.0. HRMS (ES+) calcd for $[C_{22}H_{20}N_5O_3]^+$, 402.1566; found, 402.1564.

*(1-Methyl-1H-benzo[d]imidazol-2-yl)(4-(3-morpholinopyrazin-2-yloxy)phenyl)methanone (**27**).* To a suspension of **26** (0.2 g, 0.5 mmol) in DMF was added cesium carbonate (0.2 g, 0.7 mmol) and iodomethane (0.04 mL, 0.6 mmol). The resulting mixture was stirred at room temperature overnight. The compound was precipitated from ACN/MeOH, and the resulting orange solid was filtered and rinsed with copious amounts of MeOH. The solids were dried under vacuum overnight to afford **27** (155 mg, 75% yield). ^{1}H NMR (300 MHz, DMSO-d_6) δ ppm 3.55 (d, J = 4.82 Hz, 4 H), 3.75 (br s, 4 H), 4.12 (s, 3 H), 7.38 (d, J = 8.77 Hz, 3 H), 7.43−7.54 (m, 1 H), 7.61−7.67 (m, 1 H), 7.75−7.82 (m, 1 H), 7.82−7.89 (m, 1 H), 7.97−8.06 (m, 1 H), 8.30−8.42 (m, 2 H). LC-MS m/z [M + H] 416.1.

*(1H-Benzo[d]imidazol-2-yl)(4-(3-(piperidin-1-yl)pyrazin-2-yloxy)-phenyl)methanone (**28**).* In a 50 mL round-bottom flask was placed **25** (0.1915 g, 0.546 mmol) in DMSO. Piperidine (0.270 mL, 2.73 mmol) was added, and the temperature was brought to 90 °C to stir overnight. The reaction mixture was diluted with water and extracted with CH_2Cl_2. The organic extract was washed with water and saturated NaCl and dried with $MgSO_4$. The crude product was adsorbed onto a plug of silica gel and chromatographed through a Biotage prepacked silica gel column, eluting with a gradient of 0.5−4% MeOH in CH_2Cl_2, to provide **28** (3.49 mg, 16.0% yield). ^{1}H NMR (300 MHz, $CDCl_3$) δ ppm 1.69 (br s, 6 H), 3.57 (d, J = 5.41 Hz, 4 H), 7.30 (d, J = 8.77 Hz, 2 H), 7.35−7.50 (m, 2 H), 7.54 (d, J = 2.63 Hz, 1 H), 7.60 (d, J = 7.89 Hz, 1 H), 7.94 (d, J = 2.78 Hz, 1 H), 7.98 (d, J = 8.18 Hz, 1 H), 8.87 (d, J = 8.92 Hz, 2 H). LC-MS m/z [M + H] 400.1.

*(4-(3-(1,4-Oxazepan-4-yl)pyrazin-2-yloxy)phenyl)(1H-benzo[d]-imidazol-2-yl)methanone (**29**).* A solution of **25** (0.100 g, 0.285 mmol) and homomorpholine hydrochloride (0.118 g, 0.855 mmol) in DMSO (2 mL) in a sealed tube was heated to 70 °C for 5 h. The reaction mixture was quenched with water (75 mL) and extracted with DCM (2 × 50 mL). The organic layer was washed with water (50 mL) and brine (50 mL), dried over magnesium sulfate, concentrated, and dried to give a crude product. The crude material was purified by flash column chromatography (ISCO 12 g, 0−30% EtOAc in hexane) to give **29** (8.34 mg, 70.4% yield). ^{1}H NMR (400 MHz, DMSO-d_6) δ ppm 1.95 (br s, 2 H), 3.65−3.94 (m, 8 H), 7.39 (d, J = 7.43 Hz, 4 H), 7.45−7.50 (m, 1 H), 7.61−7.89 (m, 2 H), 7.89−7.98 (m, 1 H), 8.56−8.76 (m, 2 H), 13.48 (br s, 1 H). LC-MS m/z [M + H] 416.0.

*(1H-Benzo[d]imidazol-2-yl)(4-(3-(4-methylpiperazin-1-yl)pyrazin-2-yloxy)phenyl)methanone (**30**).* In a 50 mL RBF was placed **25** (100.5 mg, 0.287 mmol) in DMSO. Methylpiperazine (151 mg, 1.43 mmol) was added, and the temperature was brought to 90 °C to stir overnight. The reaction mixture was diluted with water (15 mL) and extracted with CH_2Cl_2 (3 × 10 mL). The organic extract was washed with water (2 × 10 mL) and saturated NaCl (2× 10 mL) and dried with $MgSO_4$. The crude product was adsorbed onto a plug of silica gel and chromatographed through a Biotage prepacked silica gel column, eluting with a gradient of 0.5−8% MeOH in CH_2Cl_2, to provide **30** (3.69 mg, 31.1% yield). ^{1}H NMR (300 MHz, $CDCl_3$) δ ppm 1.43−1.74 (m, 2 H), 2.19 (d, J = 10.08 Hz, 2 H), 2.64 (s, 3 H), 2.99−3.21 (m, 2 H), 3.90 (d, J = 13.45 Hz, 2 H), 6.12 (d, J = 7.60 Hz, 1 H), 6.61 (dd, J = 6.14, 2.34 Hz, 1 H), 6.69 (d, J = 2.34 Hz, 1 H), 7.71−7.90 (m, 7 H), 8.02 (d, J = 6.14 Hz, 1 H). LC-MS m/z [M + H] 415.1.

*(1H-Benzo[d]imidazol-2-yl)(4-(3-(4-methoxypiperidin-1-yl)-pyrazin-2-yloxy)phenyl)methanone (**31**).* A suspension of **25** (75.0 mg, 0.21 mmol), 4-methoxypiperidine (73.9 mg, 0.64 mmol), and triethylamine (29.7 μL, 0.21 mmol) in DMSO (0.50 mL) in a round-bottom flask was heated to 90 °C for 1.5 h. Water (10 mL) was added to quench the reaction. Precipitates were collected by filtration and washed with water. The cake was dissolved in DCM (50 mL) and washed with water (30 mL) and brine (30 mL). The organic layer was dried over magnesium sulfate, concentrated, and dried in vacuo to give (1*H*-benzo[*d*]imidazol-2-yl)(4-(3-(4-methoxypiperidin-1-yl)pyrazin-2-yloxy)phenyl)methanone (57.2 mg, 62.3% yield). ^{1}H NMR (400 MHz, DMSO-d_6) δ ppm 13.51 (s, 1H), 8.68 (d, J = 8.6 Hz, 2H), 8.00 (d, J = 2.5 Hz, 1H), 7.87 (br s, 1H), 7.67 (br s, 1H), 7.60 (d, J = 2.5 Hz, 1H), 7.29−7.47 (m, 4H), 3.86−8.97 (m, 2H), 3.38−3.48 (m, 1H), 3.27 (s, 3H), 3.18−3.27 (m, 2H), 1.89−2.02 (m, 2H), 1.47−1.60 (m, 2H). LC-MS m/z [M + H] 430.1.

*(1H-Benzo[d]imidazol-2-yl)(4-(3-(4-hydroxypiperidin-1-yl)-pyrazin-2-yloxy)phenyl)methanone (**32**).* In a 50 mL round-bottom flask was placed **25** (154.7 mg, 0.44 mmol) in DMSO. Piperidin-4-ol (333.5 mg, 2.21 mmol) was added, and the temperature was brought to 90 °C to stir overnight. The reaction mixture was diluted with water (15 mL) and extracted with CH_2Cl_2 (3 × 10 mL). The organic extract

dx.doi.org/10.1021/jm401234w | J. Med. Chem. 2013, 56, 8781−8792

was washed with water (2 × 10 mL) and saturated NaCl (2 × 10 mL) and dried with $MgSO_4$. The crude product was adsorbed onto a plug of silica gel and chromatographed through a Biotage prepacked silica gel column, eluting with a gradient of 0.5−8% MeOH in CH_2Cl_2, to provide **32** (75.1 mg, 41% yield). ^{1}H NMR (300 MHz, $CDCl_3$) δ ppm 1.56−1.81 (m, 3 H), 1.90−2.12 (m, 2 H), 3.25 (ddd, J = 13.15, 9.94, 2.92 Hz, 2 H), 3.95 (tt, J = 8.64, 4.15 Hz, 1 H), 4.07 (dt, J = 13.30, 4.09 Hz, 2 H), 7.21−7.33 (m, 2 H), 7.41 (br s, 2 H), 7.55 (d, J = 2.78 Hz, 1 H), 7.93 (d, J = 2.78 Hz, 1 H), 8.84 (d, J = 8.92 Hz, 2 H). LC-MS m/z [M + H] 416.1. HRMS (ES+) calcd for $[C_{23}H_{22}N_5O_3]^+$, 416.1723; found, 416.1718.

*4-(3-(4-(1H-Benzo[d]imidazole-2-carbonyl)phenoxy)pyrazin-2-yl)-1-methylpiperazin-2-one (**33**).* A mixture of **25** (250 mg, 0.71 mmol), cesium carbonate (697 mg, 2.14 mmol), and 1-methylpiperazin-2-one (244 mg, 2.14 mmol) was combined in DMSO and heated to 100 °C overnight. The mixture was cooled to room temperature and diluted with H_2O and DCM. The layers were separated, and the aqueous layer was extracted with DCM (2×). The combined organics were washed with saturated NaCl solution, dried over Na_2SO_4, filtered, and concentrated. The crude residue was purified by silica gel chromatography to give **33** (34 mg, 11% yield). ^{1}H NMR (300 MHz, $CDCl_3$) δ ppm 3.05 (s, 3 H), 3.45−3.57 (m, 3 H), 3.94 (t, J = 5.26 Hz, 2 H), 4.36 (s, 2 H), 7.20−7.36 (m, 4 H), 7.38−7.48 (m, 2 H), 7.60 (d, J = 2.48 Hz, 1 H), 7.77 (br s, 2 H), 7.93 (d, J = 2.34 Hz, 1 H), 8.85 (d, J = 8.62 Hz, 2 H). LC-MS m/z [M + H] 429.0. HRMS (ES+) calcd for $[C_{23}H_{21}N_6O_3]^+$, 429.1675; found, 429.1674.

*1-(4-(3-(4-(1H-Benzo[d]imidazole-2-carbonyl)phenoxy)pyrazin-2-yl)piperazin-1-yl)ethanone (**34**).* In a 50 mL round-bottom flask was placed **25** (99.7 mg, 0.284 mmol) in DMSO. 1-(Piperazin-1-yl)ethanone (187 mg, 1.42 mmol) was added, and the temperature was brought to 90 °C to stir overnight. Reaction mixture was diluted with water (15 mL) and extracted with CH_2Cl_2 (3 × 10 mL). The organic extract was washed with water (2 × 10 mL) and saturated NaCl solution (2 × 10 mL), dried with $MgSO_4$, filtered, and concentrated. The crude product was adsorbed onto a plug of silica gel and chromatographed through a Biotage prepacked silica gel column, eluting with a gradient of 0.5−4% MeOH in CH_2Cl_2, to provide 1-(4-(3-(4-(1*H*-benzo[*d*]imidazole-2-carbonyl)phenoxy)pyrazin-2-yl)-piperazin-1-yl)ethanone (28.1 mg, 22.3% yield). ^{1}H NMR (300 MHz, $CDCl_3$) δ ppm 2.17 (s, 3 H), 3.59−3.69 (m, 6 H), 3.74−3.83 (m, 2 H), 7.31 (d, J = 8.92 Hz, 2 H), 7.43 (dd, J = 6.07, 3.00 Hz, 2 H), 7.63 (d, J = 2.63 Hz, 1 H), 7.96 (d, J = 2.78 Hz, 1 H), 8.88 (d, J = 8.92 Hz, 2 H). LC-MS m/z [M + H] 443.1. HRMS (ES+) calcd for $[C_{24}H_{23}N_6O_3]^+$, 443.1832; found, 443.1828.

*(1H-Benzo[d]imidazol-2-yl)(4-(3-(4-(2-hydroxypropan-2-yl)-piperidin-1-yl)pyrazin-2-yloxy)phenyl)methanone (**35**).* In a 50 mL round-bottom flask was placed **25** (181.4 mg, 0.517 mmol) in DMSO. 2-(Piperidin-4-yl)propan-2-ol (0.51 g, 2.59 mmol) was added, and the temperature was brought to 90 °C to stir overnight. The reaction mixture was diluted with water (15 mL) and extracted with CH_2Cl_2 (3 × 10 mL). The organic extract was washed with water (2 × 10 mL) and saturated NaCl solution (2 × 10 mL), dried with $MgSO_4$, filtered, and concentrated. The crude product was adsorbed onto a plug of silica gel and chromatographed through a Biotage prepacked silica gel column, eluting with a gradient of 0.5−4% MeOH in CH_2Cl_2, to provide **35** (0.0918 g, 38.8% yield). ^{1}H NMR (300 MHz, $CDCl_3$) δ ppm 1.21 (s, 6 H), 1.32−1.67 (m, 3 H), 1.88 (d, J = 10.52 Hz, 2 H), 2.87 (t, J = 12.06 Hz, 2 H), 4.38 (d, J = 13.15 Hz, 2 H), 7.24−7.33 (m, 3 H), 7.42 (d, J = 10.67 Hz, 2 H), 7.54 (d, J = 2.63 Hz, 1 H), 7.59 (d, J = 6.87 Hz, 1 H), 7.93 (d, J = 2.63 Hz, 1 H), 7.97 (br s, 1 H), 8.85 (d, J = 8.92 Hz, 2 H). LC-MS m/z [M + H] 458.0.

*(S)-(1H-Benzo[d]imidazol-2-yl)(4-(3-(4-(1,1,1-trifluoro-2-hydroxypropan-2-yl)piperidin-1-yl)pyrazin-2-yloxy)phenyl)methanone (**36**).* In a 50 mL round-bottom flask was placed **25** (106.3 mg, 0.303 mmol) in DMSO. (*S*)-1,1,1-Trifluoro-2-(piperidin-4-yl)propan-2-ol (198.3 g, 1.06 mmol) was added, and the temperature was brought to 90 °C to stir overnight. The reaction mixture was diluted with water (15 mL) and extracted with CH_2Cl_2 (3 × 10 mL). The organic extract was washed with water (2 × 10 mL) and saturated NaCl solution (2 × 10 mL), dried with $MgSO_4$, filtered, and concentrated. The crude product was adsorbed onto a plug of silica gel and chromatographed through a Biotage prepacked silica gel column, eluting with a gradient of 0.5−4% MeOH in CH_2Cl_2, to **36** (18.1 mg, 11.7% yield). ^{1}H NMR (300 MHz, $CDCl_3$) δ ppm 1.35 (d, J = 0.73 Hz, 3 H), 1.45−1.70 (m, 3 H), 1.81−2.09 (m, 4 H), 2.81−3.01 (m, 2 H), 4.23−4.53 (m, 2 H), 7.31 (d, J = 8.92 Hz, 2 H), 7.43 (dd, J = 6.21, 3.14 Hz, 2 H), 7.58 (d, J = 2.78 Hz, 1 H), 7.95 (d, J = 2.78 Hz, 1 H), 8.85 (d, J = 8.92 Hz, 2 H). LC-MS m/z [M + H] 512.0.

Pharmacology. *PDE10A Biochemical Assay.* Functional inhibition of human recombinant PDE10A was measured as described in the IMAP TR-FRET (time-resolved fluorescence energy transfer) assay kit protocol (Molecular Devices, Sunnyvale, CA. cat. nos. R8160, R8176, or R8159). Compound was serially diluted in 100% DMSO from a 10 mM stock and further diluted in Complete reaction buffer (10 mM Tris-HCl, pH 7.2, 10 mM $MgCl_2$, 0.05% NaN_3, 0.01% Tween 20, and 1 mM freshly added DTT) to a 4× concentration. Recombinant PDE10A enzyme and cAMP substrate were diluted in Complete reaction buffer. The optimized binding buffer was 70% binding buffer A and 30% binding buffer B. Binding reagent (1:800) and terbium donor (1: 400) were added to the binding buffer. All incubations were carried out at room temperature. Testing or control compounds (5 μL of each 4× concentration per well, 12-point dose−response curve ranging from 5.1 pM to 10 μM, tested in quadruplicate) were incubated with 5 μL of recombinant human PDE10A (0.06 units per well) in a 384-well microplate. After 30 min, 10 μL of cAMP substrate was added to each well for a final substrate concentration of 100 nM. After 1 h, 60 μL of binding buffer was added to each well. The plate was then incubated from 3 h to overnight before reading on an EnVision plate reader. The IMAP binding reagent binds to the nucleotide monophosphate generated from cyclic nucleotides (cAMP/cGMP) through phosphodiesterases and enables measurement of substrate turnover.

Permeability and Transcellular Transport. Materials. Digoxin and mannitol were purchased from Sigma-Aldrich (St. Louis, MO). ^{3}H-Digoxin and ^{14}C-mannitol were purchased from PerkinElmer Life and Analytical Sciences (Boston, MA). Transport buffer was prepared using Hank's Balanced Salt Solution (HBSS) supplemented with 10 mM Hepes, pH 7.4, and 0.1% BSA (HHBSS, Invitrogen, Grand Island, NY, BSA, Bovine Serum Albumin, Calbiochem, La Jolla, CA).

Cell Lines and Cultures. Cultures were incubated at 37 °C in a humidified (95% relative humidity) atmosphere of 5% CO_2/95% air. The parental cell line LLC-PK1 (porcine renal epithelial cells) was purchased from American Type Culture Collection (ATCC, Manassas, VA). Human MDR1 and Sprague−Dawley rat mdra1 transfectants in LLC-PK1 were generated at Amgen (Thousand Oaks, CA). Cells were cultured in Medium 199 supplemented with 2 mM L-glutamine, penicillin (50 units/mL), streptomycin (50 μg/mL), and 10% (v/v) fetal bovine serum (all from Invitrogen).[19]

Permeability and Transcellular Transport of Test Compounds. LLC-PK1, MDR1-LLC-PK1, and mdr1a-LLC-PK1 cell monolayers were seeded onto porous (1.0 μm) polycarbonate 96-well transwell membrane filters (Millipore Corp., Billerica, MA) and cultured for six days with one media replacement on day four prior to transwell experiments. Cells were washed once with warmed HHBS prior to transwell experiments. Experiments were initiated by replacing the buffer in each compartment with 0.15 mL of HBSS containing 0.1% BSA with and without 5 μM of test compound in triplicate wells. The plates were incubated for 2 h at 37 °C in an EVO incubator with shaking. Aliquots (100 μL) from both donor and receiver chambers were transferred to 96-well plates or scintillation vials. Protein was precipitated by addition of 200 μL of acetonitrile containing 0.1% formic acid and prazosin (25 ng/mL) as internal standard. After vortexing and centrifugation at 3000 rpm for 20 min, 150 μL supernatant samples were transferred to a new plate containing 50 μL of water for LC-MS/MS analysis. Transcellular transport of ^{3}H-digoxin was used as a positive control for Pgp. Paracellular permeability of ^{14}C-mannitol was used to measure the integrity of the monolayer. Sample radioactivity was measured using a liquid scintillation counter (Packard Tri-Carb 2910TR, PerkinElmer).

dx.doi.org/10.1021/jm401234w | J. Med. Chem. 2013, 56, 8781−8792

The apparent permeability coefficient (P_{app}) of all tested agents was estimated from the slope of cumulative amount (dQ) of the agent vs time (dt), and the equation:

$$P_{app} = (dQ/dt)/(A \times C_0)$$

where dQ/dt is the penetration rate of the agent (μm/s), A is the surface area of the cell layer on the Transwell (0.11 cm^2), and C_0 is the initial concentration of the test compound (μM).

LC-MS/MS RO Assays. *Animals.* All experiments were conducted under approved research protocols by Amgen's Animal Care and Use Committee (IACUC) and in accordance with National Institutes of Health Guide for Care and Use of Laboratory Animals guidelines in facilities accredited by the Association for the Assessment and Accreditation of Laboratory Animal Care (AALAC). Adult male Sprague–Dawley (SD) rats (250–280 g) were purchased from Harlan (Harlan, Indianapolis). Rats were group housed on a filtered, forced air isolation rack and maintained on sterile wood chip bedding in a quiet room on a 12 h light-dark cycle, with food and water available ad libitum. Animals were allowed for minimum 3 days of adaptation to the laboratory conditions prior to being utilized in the experiments.

LC-MS RO Assay with po Administration. Sprague–Dawley rats were pretreated with vehicle or compound via po dosing. Then 50 min after dosing, our PDE10A tracer AMG7980[15] was administered by bolus IV injection via lateral tail vein, then 10 min after tracer injection, animals under isoflurane anesthesia were euthanized by decapitation; samples of blood and brain samples were collected for analysis.

LC-MS RO Assay with ip Administration. Sprague–Dawley rats were pretreated with vehicle or compound via ip dosing. Then 20 min after dosing vehicle or compound, our PDE10A tracer AMG7980[15] was administered by bolus IV injection via lateral tail vein, and 10 min after tracer injection, animals under isoflurane anesthesia were euthanized by decapitation; samples of blood and brain samples were collected for analysis.

*Sample Analysis and Receptor Occupancy Determination of **26**, **32**, **33**, and **34**.* In both ip and po studies, striatum was used as the target tissue due to high endogenous expression of PDE10A protein, and thalamus was chosen as the reference tissue due to lower expression of PDE10A.[13]

Brain samples were weighed and HPLC-grade water was added (20% weight/volume), followed by homogenization using a Covaris E110 acoustic homogenizer (model E210, Covaris, Inc., Woburn, MA). Covaris settings: 4 °C, duty cycle 20%, intensity 8, cycles per Burst 500, treatment time 6 × 10 s. Homogenized samples were stored at −20 °C. Extraction and analysis of compound and AMG7980 tracer concentrations by API 4000 LC-MS/MS (Applied Biosystems, Carlsbad, CA).

PDE10A occupancy based on the reference tissue model was determined using the following equations:

$$BP = (STR - THA)/THA$$

$$RO\% = 100 \times [1 - (BP_{drug}/BP_{veh})]$$

where BP refers to binding potential, RO refers to receptor occupancy, BP_{drug} refers to the binding potential of the test article dosed, and BP_{veh} refers to the binding potential of the vehicle.

Note: Animals regarded as "mis-dosed" were excluded from data analysis due to experimental error during day of experiment.

Plasma Sample Preparation and Analysis. Blood was collected individually in Microtainer EDTA tubes, mixed and centrifuged at 4 °C for 10 min. The plasma sample (top aqueous phase) was then pipetted into a 96 well V-bottom plate. Plasma samples were stored at −20 °C. Extraction and analysis of compound and AMG7980 tracer concentrations by were performed by an API 4000 LC-MS/MS (Applied Biosystems, Carlsbad, CA).

Statistical Analysis. Results were expressed as the mean ± SEM (standard error of mean). Curve fit was assessed using one site-specific binding nonlinear regression on GraphPad Prism software, version 5 (GraphPad Inc., San Diego, CA).

analysis: one site − specific binding

equation: $Y = B_{max} \times X/(K_d + X)$

Rat and Human Liver Microsomal Assays. Liver microsomal stability was measured at 37 °C in phosphate buffer (66.7 mM, pH 7.4). Test compounds (1 μM) were incubated with pooled human or rat liver microsomes at 0.25 mg/mL of protein, with or without NADPH (1 mM). After 30 min, the reaction was stopped by the addition of acetonitrile containing 0.5% formic acid and internal standard. The quenched samples were centrifuged at 1650g for 20 min. The supernatants were analyzed directly for unchanged test compound using liquid chromatography and tandem mass spectrometric detection (LC-MS/MS). Intrinsic clearance was calculated based on substrate disappearance rate, assuming first-order elimination of compound over the 30 min incubation.

■ ASSOCIATED CONTENT

Ⓢ Supporting Information

Method for determination of cocrystal structures of **1** and **26** with PDE10A and summary of data collection. This material is available free of charge via the Internet at http://pubs.acs.org.

Accession Codes

The PDB ID codes for coordinates of **1** and **26** with PDE10A are 4MUW and 4MVH, respectively.

■ AUTHOR INFORMATION

Corresponding Author

*Phone: 805-313-5300. E-mail: ehu@amgen.com.

Notes

The authors declare no competing financial interest.

■ ABBREVIATIONS USED

ACN, acetonitrile; BBB, blood–brain barrier; cAMP, cyclic adenosine monophosphate; cGMP, cyclic guanosine monophosphate; ER, efflux ratio; EtOAc, ethyl acetate; HLM, human liver microsome; IPA, isopropyl alcohol; LC-MS/MS, liquid chromatography–tandem mass spectrometry; MeOH, methyl alcohol; PDE, phosphodiesterase; RLM, rat liver microsome; RO, receptor occupancy; SOC, standard of care

■ REFERENCES

(1) Schmidt, C. J.; Chapin, D. S.; Cianfrogna, J.; Corman, M. L.; Hajos, M.; Harms, J. F.; Hoffman, W. E.; Lebel, L. A.; McCarthy, S. A.; Nelson, F. R.; Proulx-LaFrance, C.; Majchrzak, M. J.; Ramirez, A. D.; Schmidt, K.; Seymour, P. A.; Siuciak, J. A.; Tingley, F. D., III; Williams, R. D.; Verhoest, P. R.; Menniti, F. S. Preclinical characterization of selective phosphodiesterase 10A inhibitors: a new therapeutic approach to the treatment of schizophrenia. *J. Pharmacol. Exp. Ther.* **2008**, *325*, 681–690.

(2) Rowley, M.; Bristow, L. J.; Hutson, P. H. Current and novel approaches to the drug treatment of schizophrenia. *J. Med. Chem.* **2001**, *44*, 477–501.

(3) Miyamoto, S.; Duncan, G. E.; Marx, C. E.; Lieberman, J. A. Treatments for schizophrenia: a critical review of pharmacology and mechanisms of action of antipsychotic drugs. *Mol. Psychiatry.* **2005**, *10*, 79–104.

(4) Cantin, L.-D.; Magnuson, S.; Gunn, D.; Barucci, N.; Breuhaus, M.; Bullock, W. H.; Burke, J.; Claus, T. H.; Daly, M.; DeCarr, L.; Gore-Willse, A.; Hoover-Litty, H.; Kumarasinghe, E. S.; Li, Y.; Liang, S. X.; Livingston, J. N.; Lowinger, T.; MacDougall, M.; Ogutu, H. O.; Olague, A.; Otto-Morgan, R.; Schoenleber, R. W.; Tersteegen, A.; Wickens, P.; Zhang, Z.; Zhu, J.; Zhu, L.; Sweet, L. PDE10A inhibitors as insulin secretagogues. *Bioorg. Med. Chem. Lett.* **2007**, *17*, 2869–2873.

(5) Chappie, T. A.; Humphrey, J. M.; Allen, M. P.; Estep, K. G.; Fox, C. B.; Lebel, L. A.; Liras, S.; Marr, E. S.; Menniti, F. S.; Pandit, J.; Schmidt, C. J.; Tu, M.; Williams, R. D.; Yang, F. V. Discovery of a series of 6,7-dimethoxy-4-pyrrolidylquinazoline PDE10A inhibitors. *J. Med. Chem.* **2007**, *50*, 182−185.
(6) Kehler, J.; Ritzén, A.; Greve, D. R. The potential therapeutic use of phosphodiesterase 10 inhibitors. *Expert Opin. Ther. Pat.* **2007**, *17*, 147−158.
(7) Höfgen, N.; Stange, H.; Schindler, R.; Lankau, H.-J.; Grunwald, C.; Langen, B.; Egerland, U.; Tremmel, P.; Pangalos, M. N.; Marquis, K. L.; Hage, T.; Harrison, B. L.; Malamas, M. S.; Brandon, N. J.; Kronbach, T. Discovery of imidazo[1,5-*a*]pyrido[3,2-*e*]pyrazines as a new class of phosphodiesterase 10A inhibitors. *J. Med. Chem.* **2010**, *53*, 4399−4411.
(8) Kehler, J.; Ritzen, A.; Langgård, M.; Petersen, S. L.; Farah, M. M.; Bundgaard, C.; Christoffersen, C. T.; Nielsen, J.; Kilburn, J. P. Triazoloquinazolines as a novel class of phosphodiesterase 10A (PDE10A) inhibitors. *Bioorg. Med. Chem. Lett.* **2011**, *21*, 3738−3742.
(9) Helal, C. J.; Kang, Z.; Hou, X.; Pandit, J.; Chappie, T. A.; Humphrey, J. M.; Marr, E. S.; Fennell, K. F.; Chenard, L. K.; Fox, C.; Schmidt, C. J.; Williams, R. D.; Chapin, D. S.; Siuciak, J.; Lebel, L.; Menniti, F.; Cianfrongna, J.; Fonseca, K. R.; Nelson, F. R.; O'Connor, R.; MacDougall, M.; McDowell, L.; Liras, S. Use of structure-based design to discover a potent, selective, in vivo active phosphodiesterase 10A inhibitor lead series for the treatment of schizophrenia. *J. Med. Chem.* **2011**, *54*, 4536−4547.
(10) Nishi, A.; Kuroiwa, M.; Miller, D. B.; O'Callaghan, J. P.; Bateup, H. S.; Shuto, T.; Sotogaku, N.; Fukuda, T.; Heintz, N.; Greengard, P.; Snyder, G. L. Distinct roles of PDE4 and PDE10A in the regulation of cAMP/PKA signaling in the striatum. *J. Neurosci.* **2008**, *28*, 10460−10471.
(11) Seeger, T. F.; Bartlett, B.; Coskran, T. M.; Culp, J. S.; James, L. C.; Krull, D. L.; Lanfear, J.; Ryan, A. M.; Schmidt, C. J.; Strick, C. A.; Varghese, A. H.; Williams, R. D.; Wylie, P. G.; Menniti, F. S. Immunohistochemical localization of PDE10A in the rat brain. *Brain Res.* **2003**, *985*, 113−126.
(12) Lakics, V.; Karran, E. H.; Boess, F. G. Quantitative comparison of phosphodiesterase mRNA distribution in human brain and peripheral tissues. *Neuropharmacology* **2010**, *59*, 367−374.
(13) Soderling, H.; Bayuga, J.; Beavo, A. Isolation and characterization of a dual-substrate phosphodiesterase gene family: PDE10A. *Proc. Natl. Acad. Sci. U. S. A.* **1999**, *96*, 7071−7076.
(14) Conti, M.; Beavo, J. Biochemistry and physiology of cyclic nucleotide phosphodiesterases: essential components in cyclic nucleotide signaling. *Annu. Rev. Biochem.* **2007**, *76*, 481−511.
(15) Hu, E.; Ma, J.; Biorn, C.; Lester-Zeiner, D.; Cho, R.; Rumfelt, S.; Kunz, R. K.; Nixey, T.; Michelsen, K.; Miller, S.; Shi, J.; Wong, J.; Della Puppa, G. H.; Able, J.; Talreja, S.; Hwang, D.-H.; Hitchcock, S. A.; Porter, A.; Immke, D.; Allen, J. R.; Treanor, J.; Chen, H. Rapid identification of a novel small molecule phosphodiesterase 10A (PDE10A) tracer. *J. Med. Chem.* **2012**, *55*, 4776−4787.
(16) Hitchcock, S. A.; Pennington, L. D. Structure−brain exposure relationships. *J. Med. Chem.* **2006**, *49*, 7559−7583.
(17) Rzasa, R. M; Hu, E.; Rumfelt, S.; Chen, N.; Andrews, K. L.; Chmait, S.; Falsey, J. R.; Zhong, W.; Jones, A. D.; Porter, A.; Louie, S. W.; Zhao, X.; Treanor, J. S.; Allen, J. R. Discovery of selective biaryl ethers as PDE10A inhibitors: improvement in potency and mitigation of Pgp-mediated efflux. *Bioorg. Med. Chem. Lett.* **2012**, *22*, 7371−7375.
(18) Wang, H.; Liu, Y.; Hou, J.; Zheng, M.; Robinson, H.; Ke, H. Structural insight into substrate specificity of phosphodiesterase 10. *Proc. Nat. Acad. Sci. U. S. A.* **2007**, *104*, 5782−5787.
(19) Schinkel, A. H.; Wagenaar, E.; van Deemter, L.; Mol, C. A. A. M.; Borst, P. Absence of the mdr1a P-glycoprotein in mice affects tissue distribution and pharmacokinetics of dexamethasone, digoxin, and cyclosporin A. *J. Clin. Invest.* **1995**, *96*, 1698−1705.